75

GA–A22786

CONF-971103--

SCALING STUDIES OF THE H–MODE PEDESTAL

by
R.J. GROEBNER and T.H. OSBORNE

JANUARY 1998

GENERAL ATOMICS

DISCLAIMER

GA–A22786

SCALING STUDIES OF THE H–MODE PEDESTAL

by
R.J. GROEBNER and T.H. OSBORNE

This is a preprint of an invited paper presented at the Thirty-Ninth Annual Meeting of the Division of Plasma Physics, November 17–21, 1997, in Pittsburgh, Pennsylvania and to be published in *Phys. Plasmas.*

Work supported by
the U.S. Department of Energy under
Contract No. DE-AC03-89ER51114

GA PROJECT 3466
JANUARY 1998

ABSTRACT

The structure and scaling of the H–mode pedestal are examined for discharges in the DIII–D tokamak [Plasma Phys. and Contr. Fusion Research (International Atomic Energy Agency, Vienna, 1986) p. 159]. For typical conditions, the pedestal values of the ion and electron temperatures T_i and T_e are comparable. Measurements of main ion and C^{6+} profiles indicate that the ion pressure gradient in the barrier is 50%–100% of the electron pressure gradient for deuterium plasmas. The magnitude of the pressure gradient in the barrier often exceeds the predictions of infinite-n ballooning mode theory by a factor of two. Moreover, via the bootstrap current, the finite pressure gradient acts to entirely remove ballooning stability limits for typical discharges. For a large dataset, the width of the pressure barrier δ is best described by the dimensionless scaling $\delta/R \propto \left(\beta_{pol}^{ped}\right)^{0.4}$ where $\left(\beta_{pol}^{ped}\right)$ is the pedestal value of poloidal beta and R is the major radius. Scalings based on the poloidal ion gyroradius or the edge density gradient do not adequately describe overall trends in the data set and the propagation of the pressure barrier observed between edge-localized modes. The width of the T_i barrier is quite variable and is not a good measure of the width of the pressure barrier.

I. INTRODUCTION

In 1982, it was discovered that, with sufficient heating power, discharges in tokamaks would exhibit a spontaneous transition from a regime of confinement called low-mode (L–mode) to a regime of markedly improved confinement called high-mode (H–mode).[1] Subsequently, it was discovered that a region of steep gradients in temperature and density existed at the very edge of the H–mode plasma.[2,3] This region is called the H–mode transport barrier because it is a result of a dramatic reduction in local heat and particle transport at the plasma boundary. The height of the transport barrier at the point where it connects to the more gentle gradients of the core plasma is called the pedestal. Certainly, the transport barrier is of interest from the point of view of basic plasma physics. It is also of interest from a pragmatic point of view because the confinement of the core plasma is clearly correlated with the height of the pedestal in the plasma pressure.[4,5] Moreover, predictions of transport models[6] suggest the pedestal value of ion temperature will provide a boundary condition which will have a major impact on the performance of the International Tokamak Experimental Reactor (ITER).[7]

Extensive studies show that a highly sheared radial electric field E_r exists in the transport barrier and much theoretical and experimental work suggests that the sheared E_r causes the improved confinement.[8,9] Nevertheless, a predictive model for the height and width of the H–mode transport barrier does not yet exist and the goal of the paper is to present an empirical study of the structure of the barrier and of the scaling of its height and width as observed in the DIII–D[10] tokamak. The results presented here extend the work reported in References 5 and 11.

For the analysis presented here, the edge profiles are fit with a hyperbolic function so that the profiles can be parameterized in terms of physically meaningful quantities as described in Section II. In Section III, these fits are used to examine the structure of the transport barrier and to compare the transport barriers in temperature, density and pressure for the ions and electrons. The scaling and magnitude of the pressure gradient in the transport barrier are compared with ballooning mode theory in Section IV and Section IV also presents empirical scalings for the width of the transport barrier in pressure. The summary and conclusions are presented in Section V.

II. MEASUREMENT AND ANALYSIS TECHNIQUES

The edge electron profiles (T_e, n_e and pressure p_e) presented here were obtained with the DIII–D multipulse Thomson scattering system[12] (TS) which has a high density of chords spanning the transport barrier and obtains data every 6–7 ms throughout a typical discharge. This system is oriented along a vertical chord and has an effective spatial separation between measurement points at the midplane of about 0.75 cm when measurements are mapped along field lines. The edge ion profiles are obtained with a multichord charge exchange recombination (CER) spectroscopy system which has a high density of chords with a minimum separation of 0.3 cm oriented along the midplane and these chords typically span the H–mode transport barrier.[13] For the data presented here, the temporal resolution varied between 2.0 ms and 10 ms. The CER system views the C VI 5290.5 Å or He II 4685.7 Å lines produced by charge transfer with a neutral beam and thus provides information of temperature, density and pressure (T_i, n_i and p_i) of the measured species (respectively, C^{6+} and He^{++}). The spatial resolution of both the TS and CER systems is quite good and allows the measurement of narrow transport barriers.

A fitting function which uses a hyperbolic tangent function (tanh) with appropriate linear terms (Fig. 1) has been found to provide an excellent fit to most H–mode edge profiles observed with the TS and CER systems.[14] A major advantage of this approach is that the parameters of the fit have a strong intuitive appeal and provide a quantitative way to measure interesting characteristics of the pedestal. For example, the value of the pedestal, the width of the transport barrier and the location of the barrier are all obtained directly from parameters in the fit. In addition, the

gradient in the middle of the transport barrier is readily obtained from the fit. For this work, the tanh functional form has empirically been found to provide a good description of edge profiles. Modeling work by Wagner and Lackner[15] suggests that the tanh form may be the natural shape of edge electron density profiles.

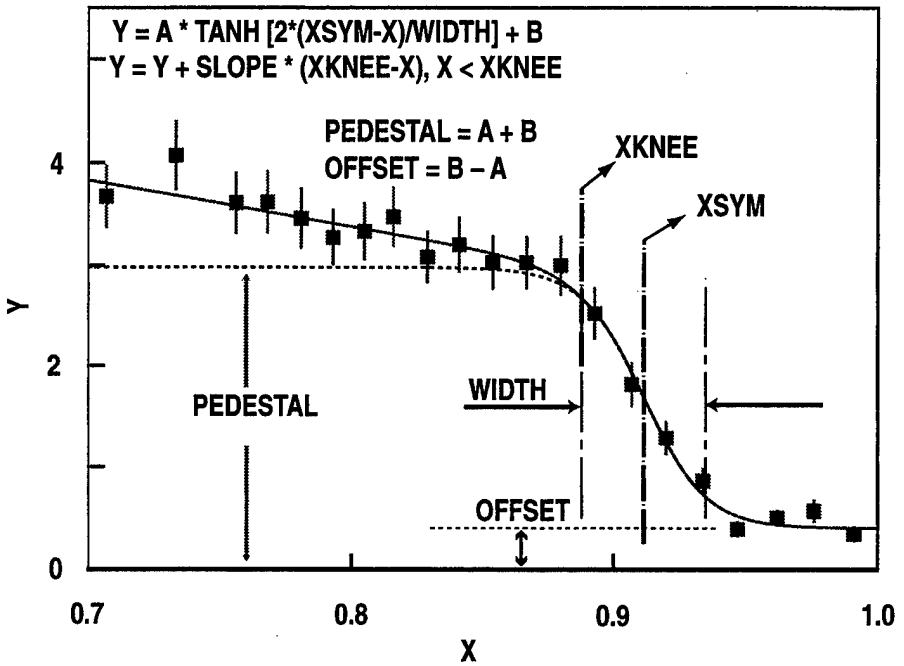

Fig. 1. Definition of fit function based on hyperbolic tangent (tanh) function. Squares show experimental points for some quantity Y as a function of some spatial coordinate X. Solid line is fit of full function to the data; dashed line is contribution of tanh to the fit.

III. PEDESTAL STRUCTURE

For typical H–mode discharges, the evidence suggests that the transport barriers for electrons and main ions, particularly the density and pressure barriers, tend to be similar in shape and magnitude. Figure 2 shows experimental data and the fits to the data for temperature, density and pressure profiles of electrons and He main ions in a helium discharge. A helium plasma was used for this measurement because the CER technique can be readily used to make measurements of He^{++} ions. In contrast, CER edge measurements of D^+ ions in deuterium plasmas are technically difficult due to interference from recycling deuterium atoms. The electron profiles, which are experimentally obtained along a vertical chord in the plasma, have been mapped with a magnetic reconstruction to the outboard midplane where the He^{++} profiles were measured. The pedestal values of T_i and T_e are equal with T_i having a shallow gradient and remaining considerably higher than T_e in the transport barrier. The relative shape of the He^{++} density profile is obtained from an intensity calibration applied to the signal amplitudes and the magnitude is scaled to the n_e profile. Neutral beam attenuation is very small in the region of interest and is not taken into account in computing the relative He^{++} density and pressure profiles. Although the shape of the n_e and n_i (main ion) profiles are quite similar, they do not quite coincide in Fig. 2. However, small systematic errors in the magnetic mapping (of order 5 mm) and possible systematic errors in diagnostic spatial calibrations (a few mm) can easily explain this discrepancy. Thus, these data are consistent with the supposition that the n_e and n_i transport barriers are very similar, as is expected unless there is an exceptionally high edge impurity content. The net result of the

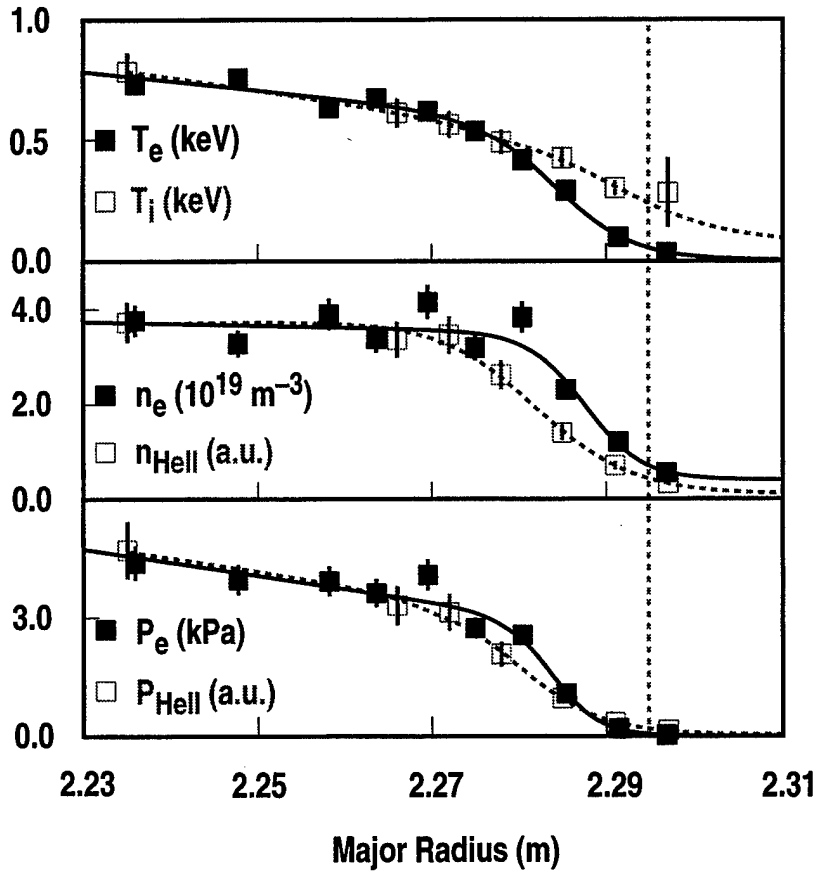

Fig. 2. Comparison of edge temperature, density and pressure data for main ions and electrons in a helium plasma. Solid (dashed) lines are fits of hyperbolic tangent function to electron (ion) data.

temperature and density profiles is that the main ions exhibit a pressure gradient in the transport barrier which is 30-40% less than that of the electrons.

Time histories of the barrier parameters for the electrons and the He^{++} ions support the idea that electrons and main ions have similar parameters. Figure 3 shows that the ion and electron pedestal values for temperature, density and pressure track quite well as a function of time in an H–mode discharge. For these data, the main ion density and pressure are scaled to match the electron data at one time. Also, due to the fact that the T_i gradient tends not to be very steep, the pedestal values obtained for the T_i fits tend to have significant variability. A more reliable measure of the T_i

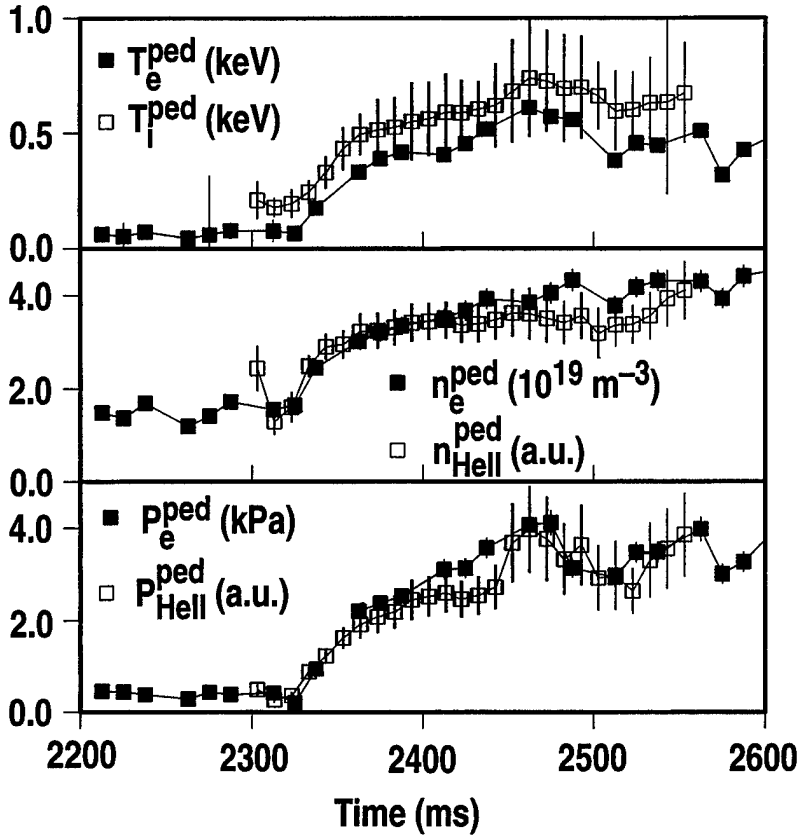

Fig. 3. Comparison of pedestal values of temperature, density and pressure data for main ions and electrons in a helium plasma as a function of time.

pedestal is the value of T_i at the innermost edge of the n_i transport barrier and that measure is displayed in Fig. 3. Figure 4 shows how the width parameters for the electron and ion barriers track during a discharge. The width for the T_i barrier tends to be higher than that of the T_e barrier. Just as the pedestal value for T_i has significant uncertainty, so does the width of the T_i barrier; simply put, the edge T_i profile does not always exhibit a well formed tanh shape. For these data, the width of the n_i profile is 30%–40% larger than the width of the n_e profile and the width of the ion pressure profile is about twice the width of the electron pressure profile.

In deuterium plasmas, numerous measurements of the C^{6+} barrier profiles (a measure of the fully ionized carbon species) tend to support the results obtained for

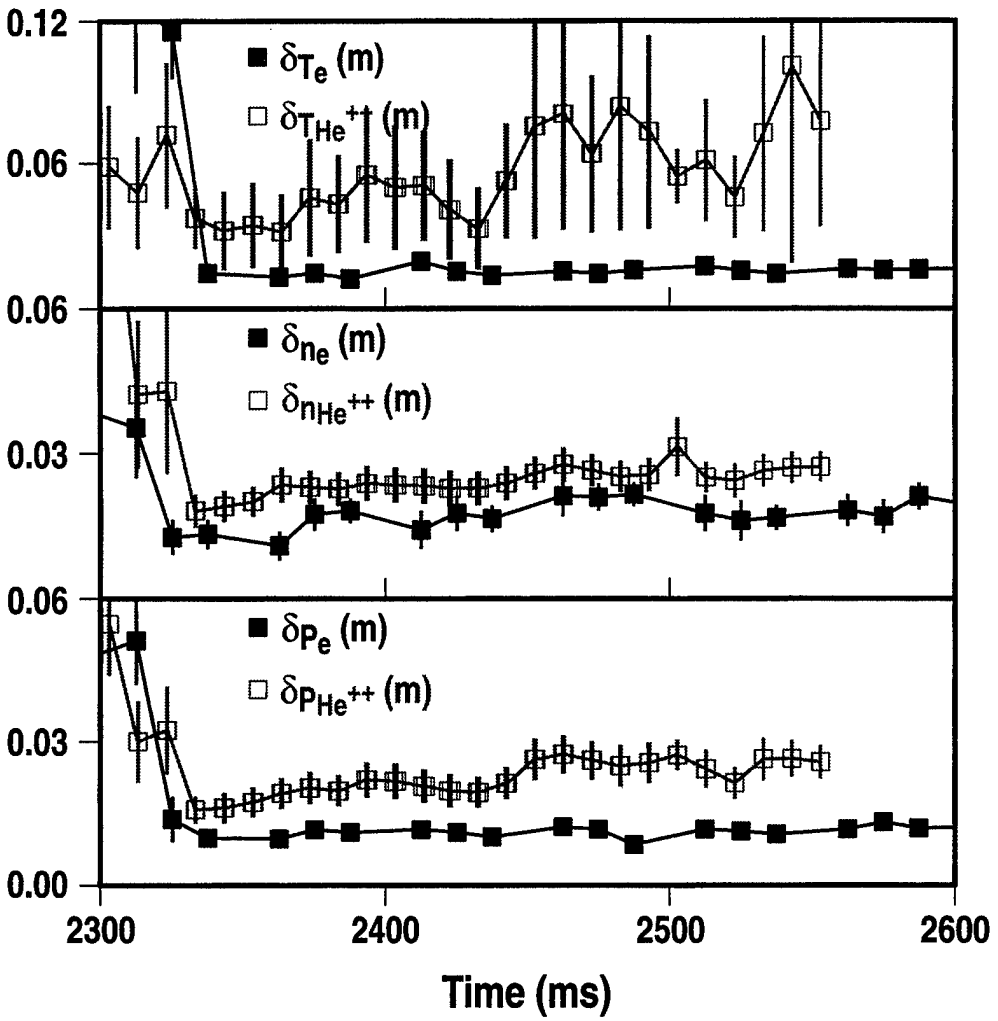

Fig. 4. Comparison of barrier width values of temperature, density and pressure data for main ions and electrons in a helium plasma as a function of time. The error bars are obtained by standard propagation of errors of the uncertainties in the measurements. When the ion temperature gradient is relatively gentle, the width of the ion temperature barrier has a large uncertainty because the barrier is not well defined in the data.

the main ions in the helium plasma. For typical DIII–D plasmas, the pedestal values of T_i and T_e are comparable and T_i has a larger barrier width parameter. There are examples in which T_i is substantially higher than T_e on the pedestal and in which the widths of the T_i and T_e barriers are equal. These correspond to hot edges (T_i = 3.5 keV on the pedestal) and suggest that the details of the T_i profile may be related to the degree of collisionality between the ions and the electrons. In contrast, the shape and location of the C^{6+} density and pressure barriers are quite similar to those

for the electron density and pressure barriers. In summary, the evidence is consistent with the idea that the edge main ions have density gradients which are similar and temperature gradients which are weaker than those of the electrons. Thus, the main ions are expected to have pressure gradients in the range of 50-100% of those of the electrons.

IV. PEDESTAL SCALING

A. Scaling with global parameters

It is desirable to have a predictive capability for the pedestal value of temperature or pressure T^{PED} or P^{PED} (where these quantities are assumed to be equal for ions and electrons). For a dataset consisting of a wide variety of DIII–D discharges, it has been shown that T^{PED} and P^{PED} must be functions of local edge parameters because they do not correlate with any of the standard global control parameters such as plasma current I_p, toroidal field B_t, line-averaged density $\langle n_e \rangle$ or heating power P_{heat}.[16] In contrast, there is a good correlation between the density pedestal n^{PED} and density $\langle n_e \rangle$ because the density is on average flat in DIII–D H–mode discharges. Furthermore, there are reasons to suspect that the total pressure gradient dP/dr can be predicted from theory. Thus, the approach taken in this paper is to search for a scaling of P^{PED} by separately examining the scalings of the gradient dP/dr and the pressure width δ under the ansatz that $P^{PED} = \delta * dP/dr$. If P^{PED} can be determined in this way, then knowledge of $\langle n_e \rangle$ will provide the value of T^{PED}. The data presented are for deuterium discharges which exhibit type I edge localized modes (ELMs). Discharges with type III ELMs are not studied in this paper.

B. Scaling of pressure gradient in barrier

There is a significant body of evidence which suggests that the attainable pressure gradient is limited by infinite-n ideal ballooning modes.[17,18] In contrast,

the process which causes an ELM may involve an additional instability. For instance, a model in which the type I ELM is caused by the coupling between ballooning modes and a low-n instability such as a kink is consistent with a number of experimental observations.[18] The focus of this paper is on the physics which limits the pressure gradient rather than on the physics which triggers ELMs.

Theory predicts that the stability of the plasma to ballooning modes depends on the interplay between the normalized pressure gradient α_{MHD}, the magnetic shear s and the safety factor q.[19] The ballooning parameter for general magnetic geometry α_{MHD} is defined as $\alpha_{MHD} = 2\mu_0(dp/d\psi)(dV/d\psi)[V/(2\pi^2 R)]^{1/2}/4\pi^2$ where p is the total plasma pressure, ψ the label for poloidal flux, V is the volume of a flux surface, R is the major radius and μ_0 is the permeability constant. For sufficiently low values of the shear s, the plasma is stable to ballooning modes for all values of α_{MHD}. However, for typical values of s at the edge of a tokamak, there is a critical value of the ballooning parameter α_{MHD}^{crit}, also called the first stability limit, above which the plasma is unstable to the ballooning modes. For values of α_{MHD} sufficiently larger than α_{MHD}^{crit}, diamagnetic effects provide stability to these modes and the plasma is in the "second stable" regime.

In order to study the scaling of dP/dr and δ, a database consisting of parameters from the tanh analysis of electron pressure profiles, plasma equilibrium values as obtained from the code EFIT[20] and values of α_{MHD}^{crit} as obtained from the ballooning stability code BALOO[21] has been assembled.[5] The database is obtained for discharges made in the ITER[7] cross sectional shape and for which the safety factor at the 95% flux surface q_{95} is in the range 3–6, the plasma current I_p is in the range 0.75–1.5 MA, the toroidal magnetic field B_t is in the range 1–2 T, the ratio of heating power to surface area is in the range 0.06–0.3 MW/m^2 and the line-averaged

density $<n_e>$ varied from 0.2–0.7 times the Greenwald limit.[22] The data were obtained during H–mode and the timing of each timeslice with respect to the ELM cycle was recorded.

As was shown in References 5 and 11, α_{MHD}^{crit} for these discharges is independent of s/q^2 with a value of about 2.7. Furthermore, the ballooning parameter obtained from the electron pressure only α_{MHD}^{e} shows no systematic trend versus s/q^2 and thus scales as expected from ideal ballooning theory. However, the magnitude of α_{MHD}^{e} alone equals or exceeds α_{MHD}^{crit}. Thus, with the ion pressure included, the magnitude of the total α_{MHD} typically exceeds α_{MHD}^{crit} by a factor of 1.5 to 2. Ballooning stability analysis performed on standard equilibria for these discharges indicates that edge of these discharges should be unstable to infinite-n ballooning modes. These results raise the question: How can the plasma exist in a region of instability?

The answer to this question appears to be that the finite edge pressure gradient improves the edge stability. When realistic edge current density profiles are used to produce model equilibria, it is found that the bootstrap current driven by the large pressure gradient can remove the stability limit imposed by ballooning modes.[23] This effect is seen in the analysis of the experimental data. As is shown in Fig. 5, typical stability analyses (as used to generate Fig. 3 in Reference 5) are based on current density J profiles obtained from magnetic diagnostics only. These J profiles tend to be flat at the edge and are inconsistent with the expectation that the large edge pressure gradients in H–mode should drive substantial edge bootstrap currents. Figure 5(b) shows that when the edge pressure gradient is forced to a more realistic shape that the equilibrium analysis produces a large edge J. When the ballooning stability analysis is done with this more realistic equilibrium, it is found that

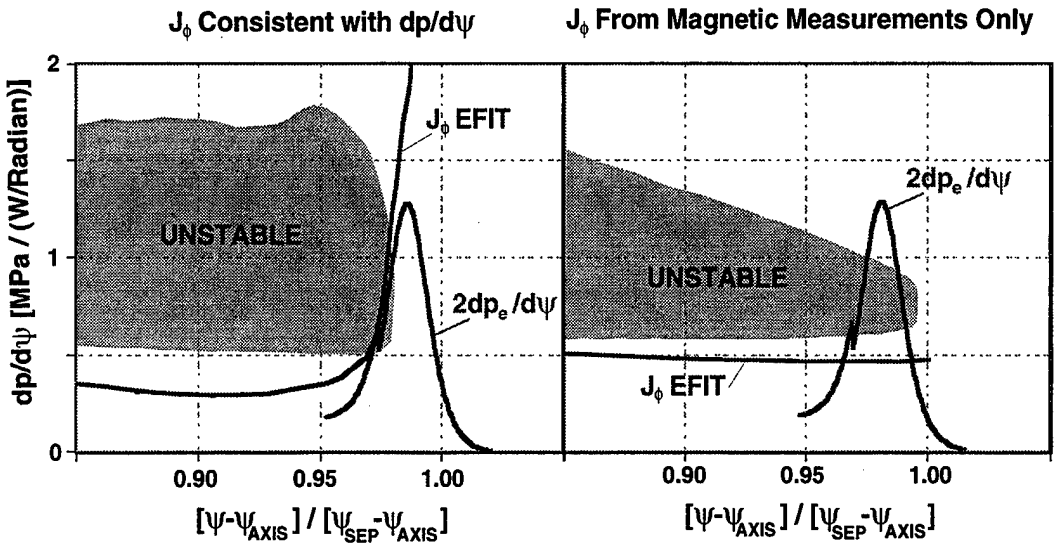

Fig. 5. Right panel shows that current density J_Φ, as determined from magnetics only, is flat at the plasma edge for an H–mode equilibrium. Stability analysis shows that this implies that a region of instability (shaded region) exists at edge and that experimental pressure gradient (taken as twice $dP_e/d\psi$) is in second stable region. Left panel shows that edge J_Φ is actually very large when it is forced to be consistent with experimental pressure gradient. Stability analysis shows that with this profile the plasma is stable to ballooning modes in region of large pressure gradient. The coordinate ψ labels the poloidal flux, ψ_{sep} refers to ψ at the separatrix and ψ_{axis} refers to ψ at the magnetic axis.

ballooning stability limits are entirely removed at the edge and thus the experimental observations do not violate theoretical predictions. In other words, the infinite-n ballooning mode theory does not explain the observed pressure gradients. It may be that some other mechanism, such as medium-n ballooning modes, limits the gradient or that additional physics must be added to the theory of infinite-n ballooning modes.

C. Scaling of width of pressure barrier

The empirical scaling of the width of the pressure barrier has been examined and has been guided somewhat by theoretical ideas. Several theoretical studies of transport barriers have invoked radial transport of either momentum[24,25] or of energy and particles[26,27] in order to explain the width of the edge barrier.

Reference 26 suggests that the width of the H–mode transport barrier is controlled primarily by the ionization length of neutrals and that the characteristic width should be $(dn_e/dr)^{-0.5}$, a quantity which can be examined with the edge database. In addition, general properties of electrostatic turbulence have been invoked[28] to suggest that the barrier width scales as the ion gyroradius ρ_i or possibly the ion poloidal gyroradius $\rho_{i\theta}$ and this idea has also be examined.

The edge database has been studied for correlations between the width of the electron pressure pedestal δ and other edge parameters, including parameters from the tanh analysis and from the magnetic equilibrium reconstructions. The width δ has a significant correlation only with I_p, P_e^{PED}, T_e^{PED} and dn_e/dr. There is also a strong correlation between I_p and dn_e/dr; thus, one of these parameters may be redundant. The general range of δ is 0.6–1.5 cm as measured at the outer midplane and this small range makes it difficult to find a definitive scaling for this parameter.

In terms of dimensional parameters, the following scalings are equally good in describing the data: $\delta \propto \left(P_e^{PED}\right)^{0.52} / B_p^{0.94}$ (see Fig. 2, Reference 5), $\delta \propto \left(T_e^{PED}\right)^{0.46} / B_p^{0.51}$ or $\delta \propto 1/\left(dn_e/dr\right)^{0.5}$ (see Fig. 6). This empirical relationship between δ and P_e^{PED} may seem trivial because if the pressure gradient were fixed, then an increase in δ would automatically imply an increase in P_e^{PED}. However, the pressure gradient is not fixed but varies significantly in the data set. Thus, this empirical relationship may imply that some fundamental process is at work to connect the width of the transport barrier to some function of the pressure. For example, finite pressure may play a role in controlling the width just as it appears to play a role in controlling the gradient of the transport barrier. The first two scalings can easily be cast in terms of dimensionless parameters and produce the results: $\delta/R \propto \left(\beta_{pol}^{PED}\right)^{0.4}$ (see Fig. 7) or $\delta/R \propto \left(\rho_{i\theta}^{PED}\right)^{0.67}$ (see Fig. 7) where β_{pol}^{PED} is the

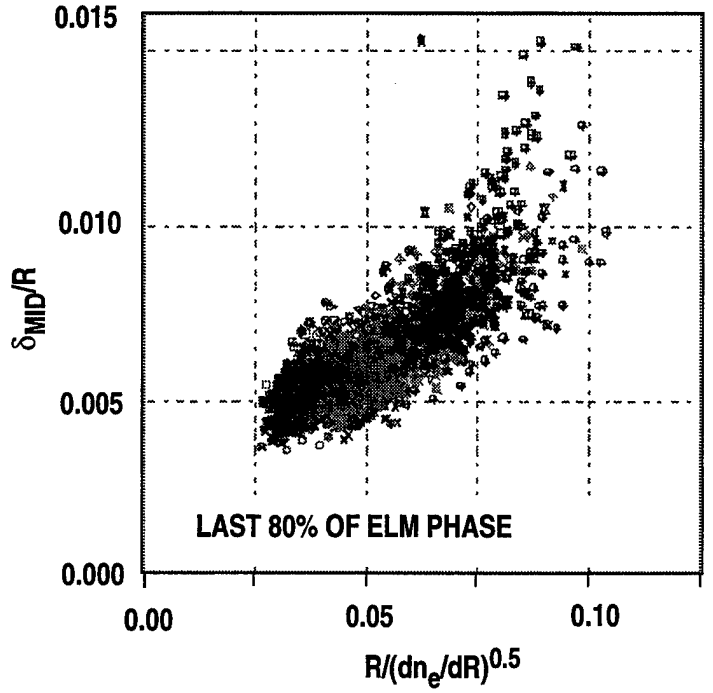

Fig. 6. Plot of pressure width δ normalized to major radius Vs sqrt(major radius divided by density gradient), a parameter proportional to ionization length in theory of Reference 26.

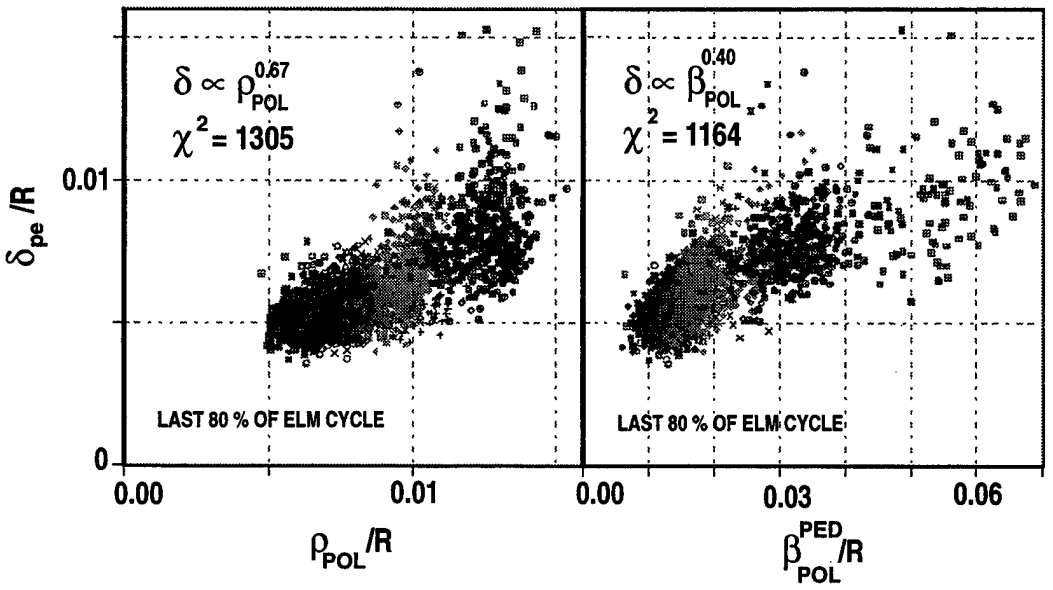

Fig. 7. Right panel shows measurements of electron pressure width δ normalized to major radius Vs electron poloidal beta. Best power law fit yields $\delta/R \propto \left(\beta_{pol}^{PED}\right)^{0.4}$. Left panel shows measurements of electron pressure width δ normalized to major radius Vs ion poloidal gyroradius normalized to R, calculated under assumption that $T_i = T_e$. Best power law fit yields $\delta/R \propto \left(\rho_{i\theta}^{PED}\right)^{0.67}$.

poloidal beta measured on the pedestal and $\rho_{i\theta}^{PED}$ is the ion poloidal gyroradius evaluated on the pedestal, under the assumption that $T_i = T_e$. From statistical grounds, the quality of these two fits is comparable and there is no reason to prefer one fit over the other.

However, under some conditions, δ increases between ELMs and this property provides a way to discriminate among the various scaling possibilities. (This phenomenon is reminiscent of the barrier front propagation discussed in Reference 27; propagation velocities of 0.2 m/s, sustained for periods of order 10 ms, have been observed.) As a result, the pressure width parameter δ exhibits changes on two different timescales. Averaged over ELMs, there is a very gradual evolution and in between ELMs, there can be more rapid changes in the width, as just described. An example will be presented for a discharge with divertor pumping which provided a decreasing edge density and a rising edge temperature during the ELMing phase of the discharge. Figure 8 shows that on a long timescale, $1/(dn_e/dr)^{0.5}$ tracks δ reasonably well but this parameter does not show a good correlation with the rapid changes in δ as seen between discharges. Figure 9 shows that no single power of T_e^{PED} matches the changes of δ. $\left(T_e^{PED}\right)^{0.3}$ matches the long term evolution of δ but not the rapid variation between ELMs whereas $\left(T_e^{PED}\right)^{1.0}$ matches the rapid change of δ between ELMs but does not match the long term evolution well. This analysis has also been done with the pedestal value of T_i and the same result was obtained. In contrast, Fig. 10 shows that $\left(P_e^{PED}\right)^{0.5}$ matches the changes of δ over both the short and long timescales. Although this analysis suggests that scalings of δ as $\left(P_e^{PED}\right)^{0.5}$ or $\left(\beta_{pol}^{PED}\right)^{0.4}$ are to be preferred, these scalings are certainly imperfect also, and some additional parameter must be important in controlling the pressure pedestal width (in order that the scatter in plots such as Fig. 7 can be reduced).

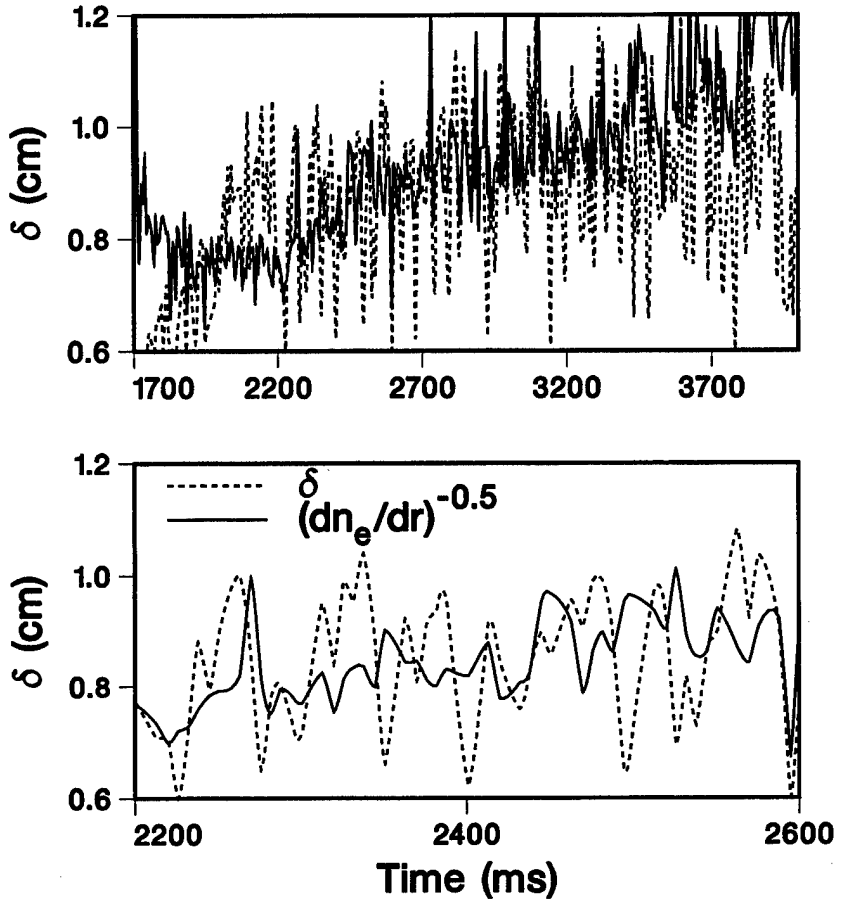

Fig. 8. In both panels, dashed line is variation of electron pressure width δ as a function of time during a discharge with divertor pumping and solid line is proportional to $(dn/dr)^{-0.5}$. The parameter $(dn/dr)^{-0.5}$ can be scaled moderately well to the long term evolution of δ (top panel) but does not fit well to rapid variation of δ between ELMs (bottom panel).

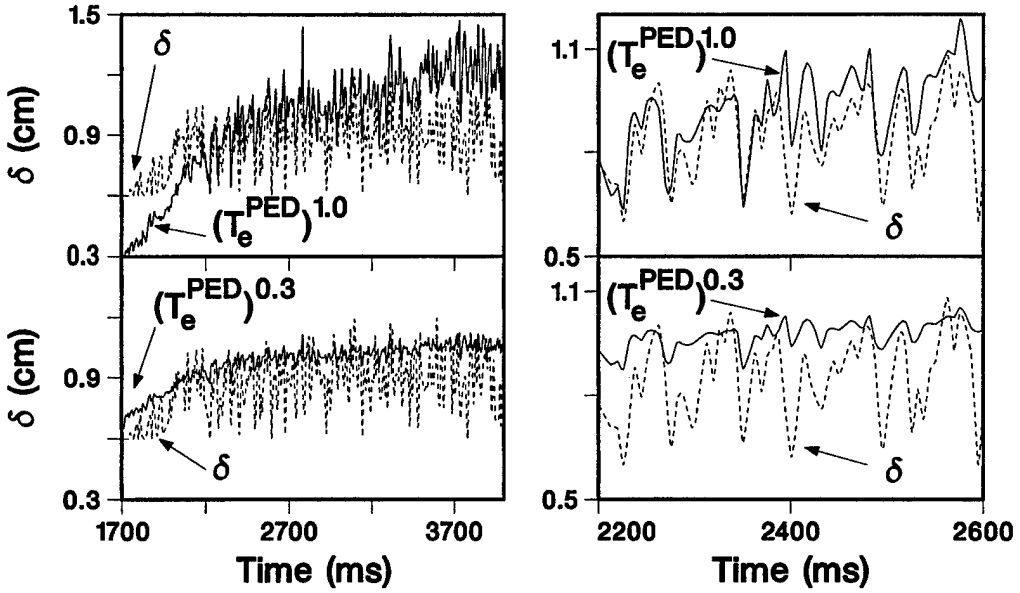

Fig. 9. Data showing that no simple function of T^{PED} can match long and short term evolution of electron pressure width δ as a function of time during a discharge with divertor pumping. Top right panel shows that evolution of δ between ELMs is matched well by $(T^{PED})^{1.0}$ and bottom left panel shows that long term evolution of δ is matched well by $(T^{PED})^{0.3}$. In contrast, top left panel shows that $(T^{PED})^{1.0}$ does not match long term evolution of δ and bottom right panel shows that $(T^{PED})^{0.3}$ does not match variation of δ between ELMs.

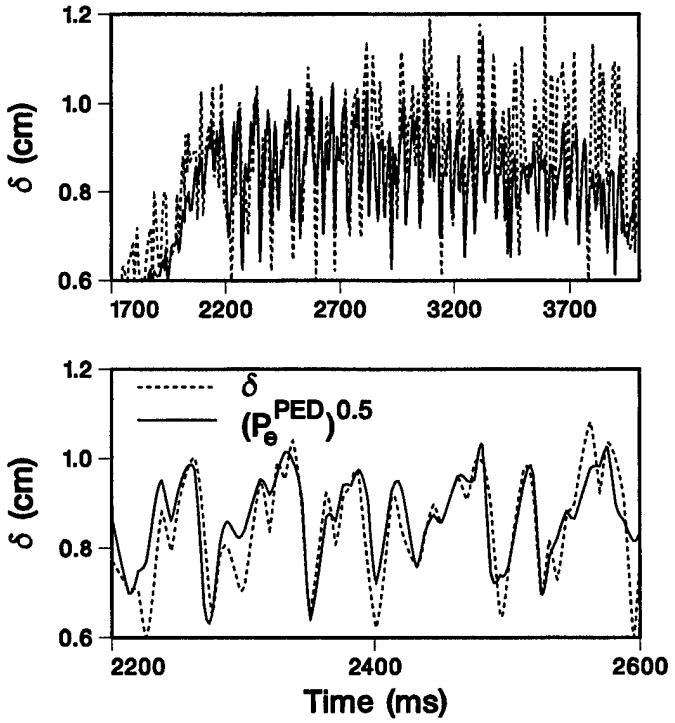

Fig. 10. Data showing that $(P^{PED})^{0.5}$ matches both the long term evolution of electron pressure width δ as a function of time during a discharge with divertor pumping (top panel) and rapid evolution of δ between ELMs (bottom panel).

V. SUMMARY AND CONCLUSIONS

This paper has reported on progress and results of studies of the H–mode pedestal in the DIII–D tokamak. A fitting procedure based on a hyperbolic tangent provides a rapid and accurate evaluation of pedestal parameters for electron and ion profiles. The pedestal values of T_i and T_e are similar for fairly standard conditions although values of T_i up to 50% higher than T_e have been observed. The width of the T_i barrier is quite variable and is not a good measure of the width of the pressure profile. Profiles of the electron and main ion density have very similar shapes. For deuterium plasmas, the edge main ion pressure gradient is most likely 50%–100% of the electron pressure gradient.

The finite pressure at the edge modifies the edge stability and can remove stability limits normally expected from ideal infinite-n ballooning modes. Nevertheless, because the observed pressure gradients scale as expected from ballooning theory and because theory can be used to predict the gradient to within a factor of about two, it seems quite plausible that the gradient is limited by some MHD phenomenon. Future work is needed to determine if medium n modes provide a stability limit in the absence of a limit from infinite-n modes or if additional physics, such as the effect of the sheared radial electric field, can modify the infinite-n ballooning theory, as required.

The width of the pressure profile is correlated with only I_p, P_e^{PED}, T_e^{PED} and dn_e/dr. A scaling going as $\left(P_e^{PED}\right)^{0.52} / B_p^{0.94}$ or equivalently as $\left(\beta_e^{PED}\right)^{0.4}$ provides the best description of the data. The physics meaning of this result is not obvious.

However, if the finite pressure gradient can modify the edge stability, perhaps it can also modify the barrier width. Under simple assumptions,[5] this scaling implies that $T^{PED} \propto RB_t/n_G^3$ where n_G is the ratio of the density to the Greenwald limit.[22] This scaling predicts a pedestal temperature of about 3.5 keV in ITER.

REFERENCES

[1]F. Wagner, G. Becker, K. Behringer, D. Campbell, A. Eberhagen, W. Engelhardt, G. Fussmann, O. Gehre, J. Gernhardt, G.v. Gierke, G. Haas, M. Huang, F. Karger, M. Keilhacker, O. Kluber, M. Kornherr, K. Lackner, G. Lisitano, G.G. Lister, H.M. Mayer, D. Meisel, E.R. Muller, H. Murmann, H. Niedermeyer, W. Poschenrieder, H. Rapp, H. Rohr, F. Schneider, G. Siller, E. Speth, A. Stabler, K.H. Steuer, G. Venus, O. Vollmer, and Z. Yu, Phys. Rev. Lett. **49**, 1408 (1982).

[2]F. Wagner, G. Fussmann, T. Grave, M. Keilhacker, M. Kornherr, K. Lackner, K. McCormick, E.R. Muller, A. Stabler, G. Becker, K. Bernhardi, U. Ditte, A. Eberhagen, O. Gehre, J. Gernhardt, G.v. Gierke, E. Glock, O. Gruber, G. Haas, M. Hesse, G. Janeschitz, F. Karger, S. Kissel, O. Kluber, G. Lisitano, H.M. Mayer, D. Meisel, V. Mertens, H. Murmann, W. Poschenrieder, H. Rapp, H. Rohr, F. Ryter, F. Schneider, G. Siller, P. Smeulders, F. Soldner, E. Speth, K. H. Steuer, Z. Szymanski, and O. Vollmer, Phys. Rev. Lett. **53**, 1453 (1984).

[3]S.M. Kaye, M.G. Bell, K. Bol, D. Boyd, K. Brau, D. Buchenauer, R. Budny, A. Cavallo, P. Couture, T. Crowley, D.S. Darrow, H. Eubank, R.J. Fonck, R. Goldston, B. Grek, K.P. Jaehnig, D. Johnson, R. Kaita, H. Kugel, B. Leblanc, J. Manickam, D. Manos, D. Mansfield, E. Mazzucato, R. McCann, D. McCune, K. McGuire, D. Mueller, A. Murdock, M. Okabayshi, K. Okano, D.K. Owens, D.E. Post, M. Reusch, G.L. Schmidt, S. Sesnic, R. Slusher, S. Suckewer, C. Surko, H. Takahashi, F. Tenney, H. Towner, and J. Valley, J. Nucl. Mater. **121,** 115 (1984).

[4]M. Greenwald, R.L. Boivin, F. Bombarda, P.T. Bonoli, C.L. Fiore, D. Garnier, J.A. Goetz, S.N. Golovato, M.A. Graf, R.S. Granetz, S. Horne, A. Hubbard, I.H.

Hutchinson, J.H. Irby, B. LaBombard, B. Lipschultz, E.S. Marmar, M.J. May, G.M. McCracken, P. O'Shea, J.E. Rice, J. Schachter, J.A. Snipes, P.C. Stek, Y. Takase, J.L. Terry, Y. Wang, R. Watterson, B. Welch, and S.M. Wolfe, Nucl. Fusion **37,** 793 (1997).

[5]T.H. Osborne, R.J. Groebner, L.L. Lao, A.W. Leonard, R. Maingi, R.L. Miller, G.D. Porter, D.M. Thomas, and R.E. Waltz, *Proc. Twenty-Fourth Euro. Conf. on Controlled Fusion and Plasma Physics,* Berchtesgaden, Germany, 1997, (European Physical Society) Vol 21A, 1101 (1997).

[6]J. Kinsey, *Proc. Twenty-Fourth Euro. Conf. on Controlled Fusion and Plasma Physics,* Berchtesgaden, Germany, 1997, (European Physical Society) Vol 21A, 1081 (1997)

[7]K. Tomabechi, *Plasma Physics and Controlled Nuclear Fusion Research 1990* (International Atomic Energy Agency, Vienna, 1991), Vol 32, p. 217.

[8]R.J. Groebner, Phys. Fluids B **5,** 2343 (1993).

[9]K.H. Burrell, Phys. Plasmas **4,** 1499 (1997).

[10]J.L. Luxon, R. Anderson, F. Batty, C.B. Baxi, G. Bramson, N.H. Brooks, B. Brown, B. Burley, K.H. Burrell, R. Callis, G. Campbell, T.N. Carlstrom, A.P. Colleraine, J. Cummings, L. Davis, J.C. DeBoo, S. Ejima, R. Evanko, H. Fukumoto, R. Gallix, J. Gilleland, T. Glad, P. Gohil, A. Gootgeld, R.J. Groebner, S. Hanai, J. Haskovec, E. Heckman, M. Heilberger, F.J. Helton, N. Hosogane, C.-L. Hsieh, G.L. Jackson, G. Jahns, G. Janeschitz, E. Johnson, A.G. Kellman, J.S. Kim, J. Kohli, A. Langhorn, L.L. Lao, P. Lee, S. Lightner, J. Lohr, M.A. Mahdavi, M. Mayberry, B. McHarg, T. McKelvey, R.L. Miller, C.P. Moeller, D. Moore, A. Nerem, P. Noll, T.H. Okhawa, N. Ohyabu, T.H. Osborne, D.O. Overskei, P.I. Petersen, T.W. Petrie, J. Phillips, R. Prater, J. Rawls. E.E. Reis, D. Remsen, P. Riedy, P. Rock, K. Schaubel, D.P. Schissel, J.T. Scoville, R. Seraydarian, M. Shimada, T. Shoji, B. Sleaford, J.P. Smith, Jr.,

P. Smith, T. Smith, R.T. Snider, R.D. Stambaugh, R. Stav, H. St. John, R.E. Stockdale, E.J. Strait, R. Street, T.S. Taylor, J. Tooker, M. Tupper, S.K. Wong, and S. Yamaguchi, *Plasma Physics and Controller Nuclear Fusion Research 1986* (International Atomic Energy Agency, Vienna, 1987), Vol I, P. 159.

[11]T.H. Osborne, R.J. Groebner, L.L. Lao, A.W. Leonard, R. Maingi, R. Miller, G.D. Porter, D.M. Thomas, and R.E. Waltz, "H-mode Pedestal Characteristics, ELMs, and Energy Confinement in ITER Shape Discharges on DIII–D," *Plasma Phys. and Contr. Fusion* (to be published 1997).

[12]T.N. Carlstrom, G.L. Campbell, J.C. DeBoo, R. Evanko, J. Evans, C.M. Greenfield, J. Haskovec, C.L. Hsieh, E. McKee, R.T. Snider, R. Stockdale, P.K. Trost, and M.P. Thomas, Rev. Sci. Instrum, **63** 4901 (1992).

[13]P. Gohil, K.H. Burrell, R.J. Groebner, J. Kim, W.C. Martin, E.L. McKee, and R.P. Seraydarian, *Proc. 14th IEEE/NPSS Symposium on Fusion Engineering, California, 1991*, (Institute of Electrical and Electronics Engineers, Inc., Piscataway, New Jersey), Vol 2, 1199 (1992).

[14]R.J. Groebner and T.N. Carlstrom, "Critical Edge Parameters for H–mode Transition in DIII–D," *Plasma Phys. and Contr. Fusion* (to be published 1997).

[15]F. Wagner and K. Lackner, *Physics of Plasma-Wall Interactions in Controlled Fusion* (edited by D.E. Post and R. Behrisch, published by Plenum Press, New York in cooperation with NATO Scientific Affairs Division), Series B, Physics Vol. 131, 931 (1986).

[16]P. Yushmanov, R.J. Groebner, L.L. Lao, and T.N. Carlstrom, "A Scaling for the H–mode Pedestal in DIII–D," Bull Amer. Phys. Soc. **41**, 1575 (1996).

[17]P. Gohil, M.A. Mahdavi, L.L. Lao, K.H. Burrell, M.S. Chu, J.C. DeBoo, C.L. Hsieh, N. Ohyabu, R.T. Snider, R.D. Stambaugh, and R.E. Stockdale, Phys. Rev. Lett. **61**, 1603 (1988).

[18]H. Zohm, Plasma Phys. Contr. Fusion **38**, 105 (1996).

[19]C.M. Bishop, P. Kirby, J.W. Connor, R.J. Hastie, and J.B. Taylor, Nucl. Fusion **24,** 1579 (1984).

[20]L.L. Lao, H.E. St. John, R.D. Stambaugh, A.G. Kellman and W. Pfeiffer, Nucl. Fusion **25,** 1611 (1985).

[21]R.L. Miller, Y.R. Lin-Liu, A.D. Turnbull, V.S. Chan, L.D. Pearlstein, O. Sauter, L. Villard, *Physics of Plasmas* **4**, 1062 (1997).

[22]M. Greenwald, J.L. Terry, S.M. Wolfe, S. Ejima, M.G. Bell, S.M. Kaye, and G.H. Neilson, Nucl. Fusion **28**, 2199 (1988).

[23]R.L. Miller, Y.R. Lin-Liu, T.H. Osborne, and T.S. Taylor, "Ballooning Mode Stability for Self-Consistent Pressure and Current Profiles at the H–mode Edge," *Plasma Phys. and Contr. Fusion* (to be published 1997).

[24]K. Itoh, Plasma Phys. Control. Fusion **36**, A307 (1994).

[25]V. Rozhansky and M. Tendler, Phys. Fluids B **4**, 1877 (1992).

[26]F.L. Hinton and G.M. Staebler, Phys. Fluids B **5**, 1281 (1993).

[27]P.H. Diamond, V.B. Lebedev, D.E. Newman and B.A. Carreras, Phys. Plasmas **2**, 3685 (1995).

[28]M. Kotschenreuther, W. Dorland, Q.P. Liu, G.W. Hammett, M.A. Beer, S.A. Smith, A. Bondeson, and S.C. Cowley, Fusion Energy 1996 (International Atomic Energy Agency, Vienna, 1997) Vol. 2, p. 371.

ACKNOWLEDGMENTS

This work represents the work of the entire DIII–D staff. In particular, the authors are grateful for the contributions of the DIII–D Pedestal Working Group: L.L. Lao, A.W. Leonard, R. Maingi, R.L. Miller, G.D. Porter, D.M. Thomas and R.E. Waltz. The authors appreciate the support and insights of K.H. Burrell, T.N. Carlstrom, B. Carreras, V.S. Chan, P. Diamond, M.A. Mahdavi, R.D. Stambaugh, G.M. Staebler, T.S. Taylor, P. Yushmanov and thank C.M. Greenfield and M.R. Wade for assistance with analysis details. G.D. Porter first showed that the hyperbolic tangent could be used to fit DIII–D edge profiles; B. Carreras suggested the interpretation of the parameters in this fit. This work is supported by the Department of Energy under Contract No. DE-AC03-89ER51115.

Report Number (14) GA--A22786
CONF-971103--

Publ. Date (11) 199801
Sponsor Code (18) DOE/ER, XF
UC Category (19) UC-400, DOE/ER

DOE